AGU PUBLICATIONS

JGR

Journal of Geophysical Research: Atmospheres

RESEARCH ARTICLE
10.1002/2016JD025136

Key Points:
- Anthropogenic emissions dominated the increase in winter haze days
- Meteorological parameters explained 17% of the increase
- Winds contributed the most to the decadal increase among the meteorological parameters

Correspondence to:
H. Liao,
hongliao@nuist.edu.cn

Citation:
Yang, Y., H. Liao, and S. Lou (2016), Increase in winter haze over eastern China in recent decades: Roles of variations in meteorological parameters and anthropogenic emissions, *J. Geophys. Res. Atmos.*, *121*, 13,050–13,065, doi:10.1002/2016JD025136.

Received 23 MAR 2016
Accepted 6 OCT 2016
Accepted article online 8 OCT 2016
Published online 5 NOV 2016

Increase in winter haze over eastern China in recent decades: Roles of variations in meteorological parameters and anthropogenic emissions

Yang Yang[1], Hong Liao[2,3], and Sijia Lou[1]

[1]Atmospheric Science and Global Change Division, Pacific Northwest National Laboratory, Richland, Washington, USA, [2]School of Environmental Science and Engineering, Nanjing University of Information Science and Technology, Nanjing, China, [3]Joint International Research Laboratory of Climate and Environment Change, Nanjing University of Information Science and Technology, Nanjing, China

Abstract The increase in winter haze over eastern China in recent decades due to variations in meteorological parameters and anthropogenic emissions was quantified using observed atmospheric visibility from the National Climatic Data Center Global Summary of Day database for 1980–2014 and simulated $PM_{2.5}$ concentrations for 1985–2005 from the Goddard Earth-Observing System (GEOS) chemical transport model (GEOS-Chem). Observed winter haze days averaged over eastern China (105–122.5°E, 20–45°N) increased from 21 days in 1980 to 42 days in 2014 and from 22 to 30 days between 1985 and 2005. The GEOS-Chem model captured the increasing trend of winter $PM_{2.5}$ concentrations for 1985–2005, with concentrations averaged over eastern China increasing from 16.1 $\mu g\,m^{-3}$ in 1985 to 38.4 $\mu g\,m^{-3}$ in 2005. Considering variations in both anthropogenic emissions and meteorological parameters, the model simulated an increase in winter surface-layer $PM_{2.5}$ concentrations of 10.5 (±6.2) $\mu g\,m^{-3}\,decade^{-1}$ over eastern China. The increasing trend was only 1.8 (±1.5) $\mu g\,m^{-3}\,decade^{-1}$ when variations in meteorological parameters alone were considered. Among the meteorological parameters, the weakening of winds by $-0.09\,m\,s^{-1}\,decade^{-1}$ over 1985–2005 was found to be the dominant factor leading to the decadal increase in winter aerosol concentrations and haze days over eastern China during recent decades.

1. Introduction

In recent years, eastern China has frequently experienced persistent and severe winter haze pollution episodes with high aerosol concentrations, which have affected half of the 1.3 billion people in China. During haze days, atmospheric visibility is less than 10 km because of the scattering and absorption of solar radiation by aerosols, which results in traffic jams and flight cancelations [*Wu et al.*, 2005]. High aerosol concentrations during haze days also have serious adverse effects on human health [*Fajersztajn et al.*, 2013; *Peplow*, 2014] and ecosystems [*Chameides et al.*, 1999]. *Lim et al.* [2012] showed that as a result of the increase in aerosol pollution, the deaths attributable to ambient particulate matter pollution have increased by about 10% worldwide over 1990–2010. The increase in aerosol concentrations over eastern China further influences the air quality in downwind areas, such as the North Pacific, through long-range transport of aerosols [*Yang et al.*, 2015]. Increased aerosol loading in recent decades has also contributed to the decrease in sunshine duration by 1.0% $decade^{-1}$ over 1954–1998 in China [*Kaiser and Qian*, 2002], trend in radiative forcing by $-6.6\,W\,m^{-2}\,decade^{-1}$ over 1961–2000 in China [*Che et al.*, 2005; *Liao et al.*, 2015], and trend of cooling in surface air temperature by 0.1 K $decade^{-1}$ from 1953 to 1997 over the Sichuan Basin [*Qian and Giorgi*, 2000].

The formation of winter haze over eastern China is associated with relatively high anthropogenic aerosol emissions and unusual meteorological conditions [*Sun et al.*, 2014; *Zhang et al.*, 2014]. In addition to the high emissions resulting from accelerated urbanization and rapid economic growth, stable synoptic meteorological conditions, such as strong temperature inversion in the lower troposphere, weak surface wind speed, and descending air in the planetary boundary layer, accumulate pollutants in the shallow layer and produce high concentrations of pollutants within the source regions [*Zhao et al.*, 2013; *Y. S. Wang et al.*, 2014; *Chen and Wang*, 2015; *Zheng et al.*, 2015; *Li et al.*, 2016]. The transport of pollutants from upwind areas is also an important contributor to local high aerosol concentrations [*Han et al.*, 2013; *L. T. Wang et al.*, 2014]. *Han et al.* [2013] found that the transport of pollutants from the southern to northern regions of the North China Plain leads to heavy $PM_{2.5}$ loading in Beijing. *L. T. Wang et al.* [2014] reported that emissions from northern Hebei and Beijing-Tianjin were two major regional contributors to $PM_{2.5}$ pollution in Shijiazhuang in January 2013.

Many studies have reported that eastern China has experienced an increasing trend of haze days during recent decades [*Che et al*., 2007, 2009; *Zhao et al*., 2011; *Cheng et al*., 2013; *Ding and Liu*, 2014; *Chen and Wang*, 2015]. Owing to the lack of a long-term monitoring network for aerosols in China, haze days are identified as days with visibility less than 10 km and relative humidity less than 90% based on observations, which separates haze from fog assuming that fog occurs when relative humidity is equal to or larger than 90% [*Ding and Liu*, 2014]. *Zhao et al*. [2011] reported that averaged over 16 urban sites over the Beijing-Tianjin-Hebei area in northern China, the yearly haze days increased from 46 days in 1986 to 78 days in 2007. *Chen and Wang* [2015] examined haze days at 78 sites in northern China and found that spatially averaged winter haze days increased from 16 days in 1960 to 27 days in 2012. *Cheng et al*. [2013] found that for the cities of Nanjing, Hangzhou, and Suzhou in the Yangtze River Delta in eastern China, annual haze days increased continuously from about 40, 50, and 20 days in the 1980s to 140, 160, and 70 days after 2001, respectively. *Che et al*. [2009] examined haze trends over 31 provincial capitals in China between 1980 and 2005 and showed evident increasing trends of winter haze in eastern and southwestern China and decreasing trends in northeastern and northwestern China. *Ding and Liu* [2014] also showed that haze days increased in economically developed eastern China, especially in southern China with the average annual haze days increasing from 3.9 days in the 1960s to 60 days in 2008, whereas it decreased in less economically developed northeastern and northwestern China. They also found that averaged over 553 sites in China, winter haze days increased rapidly from 1 day in the 1960s to 5 days in the 2010s.

The increase in winter haze days on the decadal timescale over eastern China is usually attributed to the increase in anthropogenic aerosol emissions that accompanies rapid urbanization and economic development. A few studies have also shown the contribution of meteorological parameters to decadal variations in haze days. *Li et al*. [2016] found negative correlation coefficients of −0.41 to −0.49 between fog-haze days and the East Asian winter monsoon indices (indices are defined based on 850 hPa winds or geopotential height) and suggested that the weakened near-surface winds in the weak East Asian winter monsoon years reduce the outflow of haze and favor the accumulation of pollutants over eastern China. This mechanism is important considering that wind speed decreased by $-0.2\ \mathrm{m\ s^{-1}}$ decade^{-1} between 1969 and 2000 [*Xu et al*., 2006]. *Ding and Liu* [2014] found that the reduction of surface relative humidity from 70% to 67% over 1961–2011 in China due to the increase in surface air temperature from 10.5 to 10.8°C might have caused the increase in yearly haze days from 4 to 15 days. Understanding the causes of the increase in haze days and aerosol concentrations is essential for long-term planning of air quality. However, few previous studies have quantitatively separated the roles of anthropogenic emissions and meteorological parameters on decadal variations in haze days over eastern China during recent decades.

Here we present a systematic investigation of the decadal trend of winter haze over eastern China during recent decades based on a set of two simulations covering the winters of 1985–2005 by a global three-dimensional Goddard Earth Observing System (GEOS) chemical transport model (GEOS-Chem) combined with observed daily atmospheric visibility and assimilated meteorological parameters. We aimed to quantify the following: (1) observed winter haze days and simulated winter $PM_{2.5}$ concentrations over eastern China during recent decades, (2) the roles of anthropogenic emissions and meteorological parameters in the trend of simulated winter $PM_{2.5}$ (sum of sulfate, nitrate, ammonium, black carbon, and organic carbon) concentrations, and (3) the relative importance of each meteorological parameter.

The GEOS-Chem model, emissions, and numerical experiments are described in section 2. Section 3 provides a comparison of the observed haze days and simulated $PM_{2.5}$ concentrations in winter over eastern China during recent decades. Section 4 investigates the roles of anthropogenic emissions and meteorological parameters in the trend of simulated winter $PM_{2.5}$ concentrations. Section 5 examines the relative importance of each meteorological parameter on the trend.

2. Data and Experimental Methods

In this work, observed visibility data were used to calculate the winter haze days and to evaluate the model's ability in simulating the trend of $PM_{2.5}$ concentrations over eastern China during recent decades. The observed visibility data were derived from the National Climatic Data Center (NCDC) Global Summary of Day (GSOD) database, which collected data from 346 meteorological stations in China between 1980 and 2014 (http://www7.ncdc.noaa.gov/CDO/cdoselect.cmd?datasetabbv=GSOD&countryabbv=&georegionabbv=). The data set

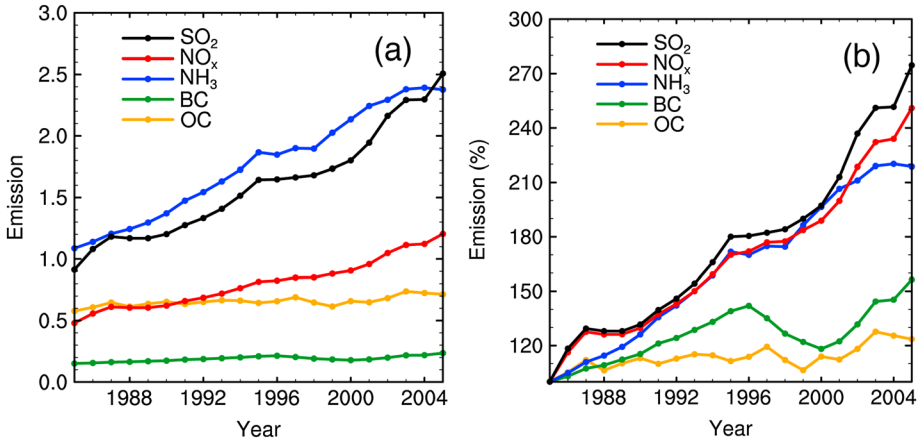

Figure 1. (a) Seasonal variations in anthropogenic plus natural emissions of sulfur dioxide (SO_2, Tg S yr^{-1}), nitrogen oxide (NO_x, Tg N yr^{-1}), ammonia (NH_3, Tg N yr^{-1}), black carbon (BC, Tg C yr^{-1}), and organic carbon (OC, Tg C yr^{-1}) averaged over eastern China (105–122.5°E, 20–45°N) in December-January-February (DJF) for 1985–2005 and (b) their percentage changes relative to 1985 values.

includes daily visibility, temperature, dew point temperature, sea level pressure, wind speed, and precipitation and has been used in many previous studies [*Chang et al*., 2009; *K. Wang et al*., 2009; *Chen and Xie*, 2012; *Deng et al*., 2012]. Only days without precipitation were analyzed in this study, which accounted for about 91% of days with observed atmospheric visibility data available. Observed haze days are defined as days with visibility less than 10 km and relative humidity less than 90% [*Chen and Xie*, 2012; *Ding and Liu*, 2014; *Chen and Wang*, 2015].

We simulated aerosols using the global chemical transport model GEOS-Chem (version 8.02.01, http://acmg.seas.harvard.edu/geos) driven by the assimilated meteorological fields from the Goddard Earth Observing System (GEOS) of the NASA Global Modeling Assimilation Office. The version of the model used here has a horizontal resolution of 2° latitude by 2.5° longitude with 30 vertical layers up to 0.01 hPa. The GEOS-Chem model has fully coupled O_3–NO_x–hydrocarbon chemistry and aerosols including sulfate, nitrate, ammonium, organic carbon, black carbon [*Park et al*., 2003; *Park*, 2004], mineral dust [*Fairlie et al*., 2007], and sea salt [*Alexander et al*., 2005]. Partitioning of nitric acid and ammonia between the gas and aerosol phases was calculated using ISORROPIA package, which performs aerosol thermodynamical equilibrium [*Nenes et al*., 1998]. Heterogeneous reactions of anthropogenic aerosols included hydrolysis of N_2O_5 [*Evans and Jacob*, 2005], irreversible absorption of NO_3 and NO_2 on wet aerosols [*Jacob*, 2000], and the uptake of HO_2 by aerosols [*Thornton et al*., 2008]. The mineral dust and sea-salt aerosols were not considered in this study, because they are not major aerosol components during winter in China based on previous measurements [*Xuan et al*., 2000; *Ye et al*., 2003; *Duan et al*., 2006]. However, excluding dust and sea salt may lead to low bias in simulated aerosol concentrations.

The performance of the GEOS-Chem model in simulating aerosols has been evaluated in many studies using ground-based measurements in China [*Zhang et al*., 2010; *Jeong and Park*, 2013; *Jiang et al*., 2013; *Wang et al*., 2013; *Lou et al*., 2014; *Y. Wang et al*., 2014; *Yang et al*., 2015]. The model underestimated $PM_{2.5}$ concentrations by a factor of 3–4 during the 2013 severe haze event [*Y. Wang et al*., 2014], which may result in low bias in the simulated $PM_{2.5}$ trend in our study. However, the model captured well the spatial distributions, seasonal and interannual variations of concentrations, and optical depth of aerosols in China [*Jiang et al*., 2013; *Yang et al*., 2015].

Global emissions of aerosols and their precursors in the GEOS-Chem model followed *Park et al*. [2003, 2004], with anthropogenic emissions of sulfur dioxide (SO_2), nitrogen oxide (NO_x), and ammonia (NH_3) in Asia overwritten by the emission inventories of *Streets et al*. [2003] and *Zhang et al*. [2009]. Interannual variations in anthropogenic emissions were represented by annual scaling factors. To simulate with anthropogenic emissions from China for the winters of 1985–2005, the scaling factors for SO_2 and NO_x followed those described in *van Donkelaar et al*. [2008]. For black carbon (BC) and organic carbon (OC), the scaling factors for 1996–2006 were taken from *Lu et al*. [2011] and those for 1985–1995 were derived from the Intergovernmental

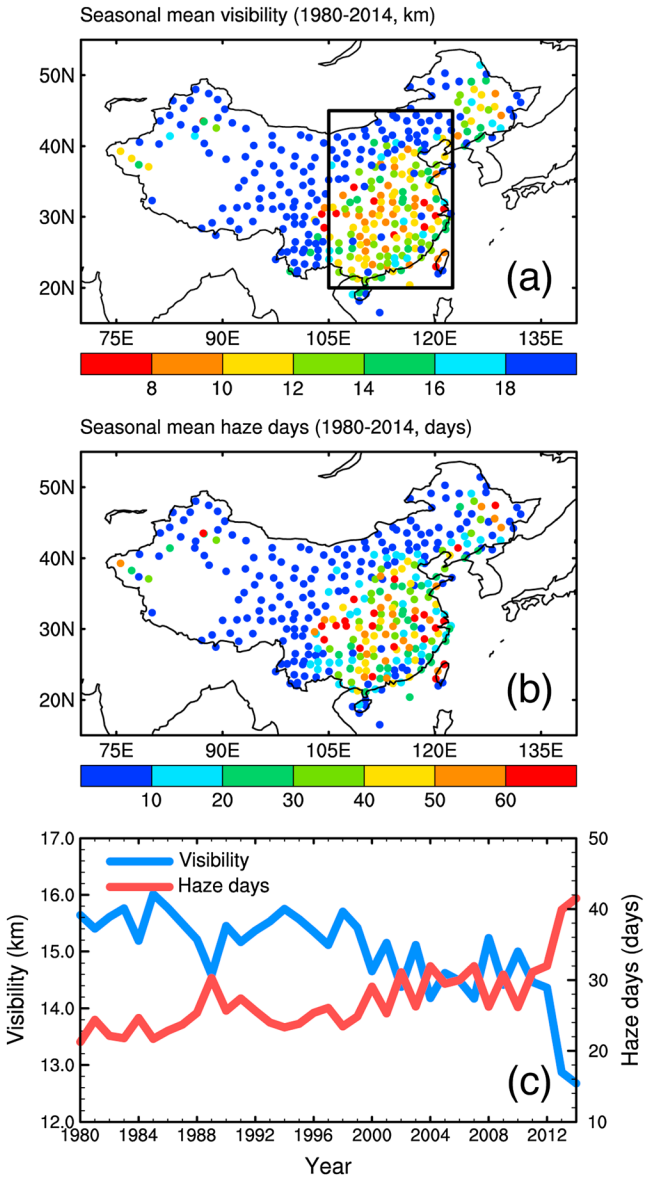

Figure 2. Spatial distribution of the observed DJF (a) atmospheric visibility (km) and (b) haze days (days) in China averaged over 1980–2014. (c) The time series of observed DJF visibility (blue line, km) and haze days (red line, days) averaged over eastern China for 1980–2014. The black box in Figure 2a (105–122.5°E, 20–45°N) shows the area selected to represent eastern China. The observed haze days are defined as days with visibility less than 10 km and relative humidity less than 90% in this study.

Panel on Climate Change (IPCC) Fifth Assessment Report (AR5) emissions inventories [*Lamarque et al.*, 2010] using a linear interpolation approach. IPCC AR5 inventories have emissions for every 10 years between 1850 and 2000. Scaling factors for NH_3 for 1994 to 2006 were obtained from *Dong et al.* [2010], and those for 1985 to 1993 were derived from the IPCC AR5 emission inventories. Biomass burning emissions were taken from the Global Fire Emissions Database, version 2, inventory and fixed at the 2005 level [*van der Werf et al.*, 2006]. Figure 1 shows the variations in December-January-February (DJF) emissions (both anthropogenic and natural emissions) of aerosols and aerosol precursors in eastern China (105–122.5°E, 20–45°N) from 1985 to 2005. Among the emissions of aerosols and aerosol precursors, SO_2 emissions showed the largest increase. Wintertime SO_2 emissions increased from 0.91 Tg S per season in 1985 to 2.51 Tg S per season in 2005 during DJF (an increase of 176% relative to the emissions in DJF of 1985). From 1985 to 2005, emissions of NO_x, NH_3, BC, and OC increased by 150, 118, 60, and 22%, respectively.

Aerosol concentrations in China for the winters of 1985 to 2005 were simulated using the GEOS-Chem model driven by GEOS-4 meteorological fields. The simulations covered 21 winter seasons, which were defined as the last month of 1 year and the following 2 months of next year. For example, winter of 2000 includes December of 2000 and January and February of 2001. The following simulations were performed to compare the trends of observed haze days and simulated $PM_{2.5}$ concentrations over eastern China in winter and to identify the roles of variations in anthropogenic emissions and meteorological parameters in the simulated $PM_{2.5}$ trend:

1. *CTRL*. Simulation of DJF aerosols from December 1985 to February 2006, with variations in both meteorological parameters and anthropogenic emissions over 1985–2006.
2. *MET*. Simulation of DJF aerosols in from December 1985 to February 2006 with variations in meteorological parameters alone to quantify the impact of variations in these parameters on the trend of simulated $PM_{2.5}$ concentrations over eastern China. Meteorological parameters were allowed to vary over 1985–2006. Anthropogenic emissions were fixed at the 2005 level.

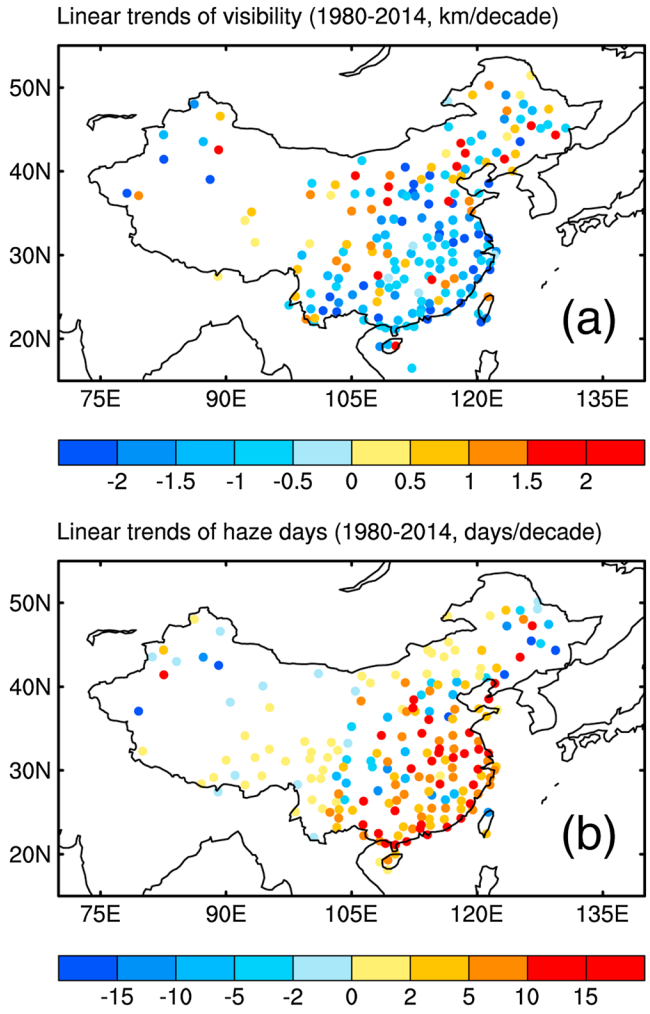

Figure 3. Spatial distributions of linear trends of (a) observed DJF mean of atmospheric visibility (km decade^{-1}) and (b) haze days (d decade^{-}) in China for 1980–2014. The trends were obtained from the linear square fit. Only stations with trends at the 5% significance level are shown in Figures 3a and 3b.

In the MET simulation, anthropogenic emissions were fixed at the 2005 level to examine the trend of aerosols caused by variations in meteorological parameters. If the emissions were set to 1985, the model may not accurately reproduce aerosol concentrations for recent modern conditions due to the nonlinearity between emissions and concentrations and would bias the simulated aerosol trends in the MET simulation.

3. Observed Haze Days and Simulated $PM_{2.5}$ Concentrations During Recent Decades

Figures 2a and 2b show the DJF mean atmospheric visibility and haze days averaged over 1980 to 2014, respectively. Observed atmospheric visibility was low in eastern China, where industries and the economy have developed quickly compared with other regions in China. The visibility was lower than 10 km at one fifth of the sites in eastern China (105–122.5°E, 20–45°N). The average visibility over eastern China was 15.0 km, which was less than the average value of 18.3 km for the whole China. Based on the definition of haze days in terms of atmospheric visibility and relative humidity in this study, the average number of haze days in DJF over eastern China was 27.2 days, which was higher than the national mean of 19.2 days.

Figure 2c presents the time series of observed DJF mean visibility and haze days over eastern China from 1985 to 2005. During the past three decades, winter visibility exhibited a significant decreasing trend over eastern China, decreasing from 15.6 km in 1980 to 14.4 km in 2012 and 12.7 km in 2014. At the same time, eastern China experienced an increasing trend of winter haze days, with 21.3, 32.0, and 41.5 days in 1980, 2012, and 2014, respectively. Linear trends of atmospheric visibility and haze days over eastern China were −0.4 km decade^{-1} and +2.6 d decade^{-1}, respectively, from 1980 to 2012, which were statistically significant at the 95th percentile. In spite of the different number of sites and different time coverage, the trends obtained in this study are comparable, to some extent, with previous studies. *Che et al.* [2007] showed that nationwide winter visibility averaged over 615 sites decreased by −1.3 km decade^{-1} between 1991 and 2005. *Chen and Wang* [2015] showed that between 1960 and 2012, winter visibility decreased from 21 to 17 km and haze days increased from 16 to 27 days when the averages over 78 sites in northern China were considered. The visibility and haze days exhibited high values after 2013, because of extremely high concentrations of aerosols in recent years [*Y. Wang et al.*, 2014; *Zhang et al.*, 2014].

Figure 3 shows the spatial distributions of the linear trends of observed DJF atmospheric visibility and haze days in China for 1980 to 2014. In the past three decades, 104 (99) of 196 sites over eastern China exhibited a

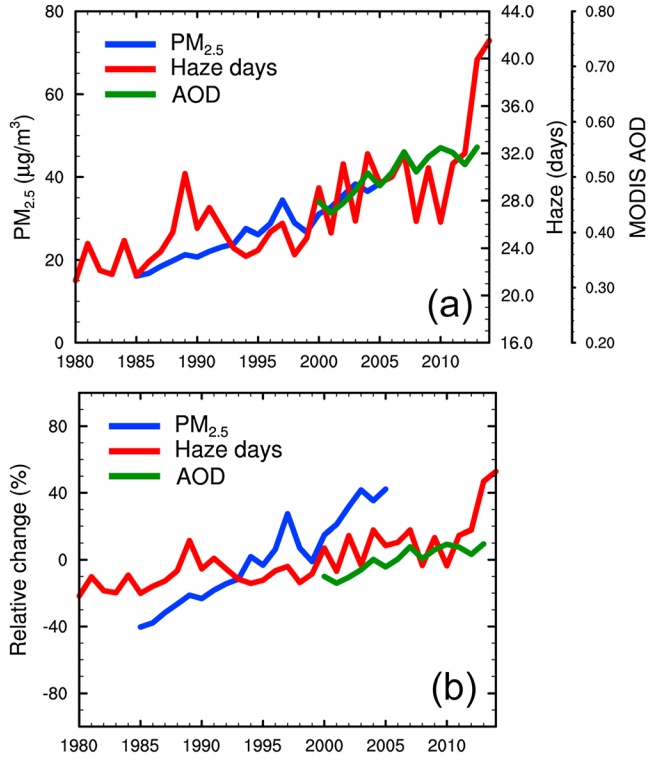

Figure 4. The time series of (a) simulated surface-layer $PM_{2.5}$ concentrations from the CTRL simulation ($\mu g\ m^{-3}$), observed haze days (days), and MODIS aerosol optical depth (AOD) averaged over 196 stations in eastern China (boxed stations in Figure 2a) in DJF for 1985–2005, 1980–2014, and 2000–2013, respectively and (b) their percentage changes relative to the mean values.

statistically significant increasing (decreasing) trend of winter haze days (visibility). Winter haze days increased with a trend of more than 15 d decade^{-1} in 17 sites over eastern China, which were mostly provincial capitals. The increase in haze days and decrease in visibility suggest that eastern China has experienced an increase in winter aerosol concentrations during the past few decades.

Figure 4a presents the observed winter haze days for 1980–2014 and simulated surface-layer $PM_{2.5}$ concentrations for 1985–2005 from the CTRL simulation averaged over 196 sites in eastern China (boxed area in Figure 2a). Over 1985–2005, the GEOS-Chem model simulated the increasing trend of $PM_{2.5}$ concentrations, increasing from 16.1 $\mu g\ m^{-3}$ in 1985 to 38.4 $\mu g\ m^{-3}$ in 2005, which agrees with the observed increases in winter haze days (from 21.7 days in 1985 to 29.5 days in 2005). Although the model may not well reproduce the interannual variations of $PM_{2.5}$ concentrations when compared with observed visibility data, probably due to the fixed biomass burning emissions in the simulations, it does not influence the main results of the variation in $PM_{2.5}$ concentrations on the decadal timescale. Owing to the time coverage limitation of the simulation, the site-averaged aerosol optical depth (AOD) at 550 nm in DJF for 2000–2013 derived from Moderate Resolution Imaging Spectrometer (MODIS) satellite data is also presented in Figure 4a. The AOD showed an increasing trend after 2000, with values increasing from 0.45 in 2000 to 0.55 in 2013, indicating that aerosol concentrations were still increasing in the past decade, while haze days and visibility became stable between 2002 and 2012. The difference between the trends of MODIS AOD and visibility results from many factors, such as relative humidity, chemical composition of aerosols, and the spatial and temporal differences between satellite and on-site observations. Also, AOD is a column amount, but visibility values are from the surface layer. The variations in aerosols are driven by both anthropogenic emissions and meteorological fields. *Yang et al.* [2015] found that the interannual variations in the aerosol outflow from East Asia were dominated by meteorological fields and that the decadal trends were mainly controlled by anthropogenic emissions. The sudden increase in haze days after 2010 (Figure 4a) was more likely due to the interannual variation, which resulted mainly from changes in meteorological parameters. Many previous studies have associated the sudden increase in haze in recent years with abnormal meteorological conditions [*Y. S. Wang et al.*, 2014; *Zhang et al.*, 2014; *Zheng et al.*, 2015]. Through a model-assisted analysis, *Zheng et al.* [2015] found that the severe winter haze in recent years was driven by stable synoptic meteorological conditions and not by an abrupt increase in anthropogenic emissions.

Figure 4b shows the percentage change in observed winter haze days, simulated $PM_{2.5}$ concentrations, and MODIS AOD, relative to the mean values. $PM_{2.5}$ concentration, haze days, and AOD increased by 80, 70, and 20% over 1985–2005, 1980–2014, and 2000–2013, respectively. Note that these variables showed different increasing trends because they were related nonlinearly to each other. The uncertainties from the satellite

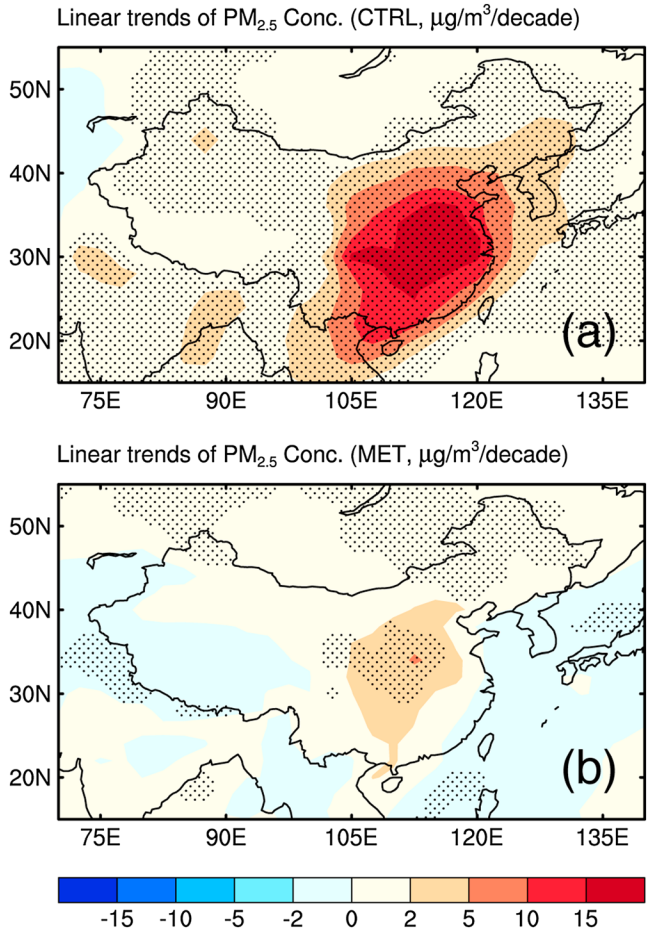

Figure 5. Linear trends of simulated surface-layer $PM_{2.5}$ concentrations ($\mu g\,m^{-3}\,decade^{-1}$) for 1985–2005 from the (a) CTRL and (b) MET simulations, respectively. The dotted areas indicate statistical significance at the 95% confidence level from the *F* test on the regression model.

AOD retrieval and the biases in GEOS-Chem vertical profiles [*van Donkelaar et al.*, 2010] may also have led to the differences in the trends.

4. Effects of Anthropogenic Emissions and Meteorological Parameters

Figure 5 shows the spatial distributions of trends of simulated DJF surface-layer $PM_{2.5}$ concentrations for 1985–2005 from the CTRL and MET simulations calculated using the linear square fit. In the CTRL simulation, $PM_{2.5}$ concentrations increased significantly over eastern China, with linear trends of up to 15 $\mu g\,m^{-3}\,decade^{-1}$ over most parts of eastern China (Figure 5a). The spatial pattern of $PM_{2.5}$ is consistent with that of the increasing trend in winter haze days (Figure 3b).

Considering the variations in meteorological parameters alone in the MET simulation, the simulated DJF $PM_{2.5}$ concentrations exhibited much smaller increasing trends (Figure 5b) compared with those in the CTRL simulation. Relatively large increasing trends were found mainly over central eastern China (105–115°E, 25–40°N), with values in the range of 2–5 $\mu g\,m^{-3}\,decade^{-1}$, indicating that in addition to anthropogenic emissions, variations in meteorological parameters alone partly resulted in the increase in winter $PM_{2.5}$ concentrations over eastern China during recent decades, and their roles are significant over central eastern China.

Figure 6a shows the time series of simulated DJF surface-layer $PM_{2.5}$ concentrations averaged over eastern China from 1985 to 2005 in the CTRL and MET simulations. Over eastern China, the simulated DJF $PM_{2.5}$ concentrations increased from 15.4 $\mu g\,m^{-3}$ in 1985 to 36.8 $\mu g\,m^{-3}$ in 2005 in the CTRL simulation, with a statistically significant trend of 10.5 (±6.2) $\mu g\,m^{-3}\,decade^{-1}$. With variations in meteorological parameters alone in the MET simulation, eastern China had a smaller increasing trend in $PM_{2.5}$ concentrations, with a statistically significant trend of 1.8 (±1.5) $\mu g\,m^{-3}\,decade^{-1}$, about 17(±14)% of the value in the CTRL simulation. These results suggest that variations in anthropogenic emissions dominated the increase in winter $PM_{2.5}$ concentrations over eastern China during recent decades. However, variations in meteorological parameters also played an important role in influencing the decadal increase in winter $PM_{2.5}$ concentrations, which contributed 17(±14)% to the increasing trend between 1985 and 2005.

Figure 6b presents the DJF mean surface-layer $PM_{2.5}$ concentrations over eastern China after linear trends of 10.5 and 1.8 $\mu g\,m^{-3}\,decade^{-1}$ were removed from the CTRL and MET simulations, respectively. Including only interannual signals, the CTRL and MET simulations exhibited the same peaks and troughs of the detrended $PM_{2.5}$ concentrations over eastern China. The similarity indicates that interannual variations of $PM_{2.5}$ concentrations were mainly driven by variations in meteorological parameters, not anthropogenic emissions. Note that the peaks in the modeled $PM_{2.5}$ concentrations in winter 1997 (December 1997 and

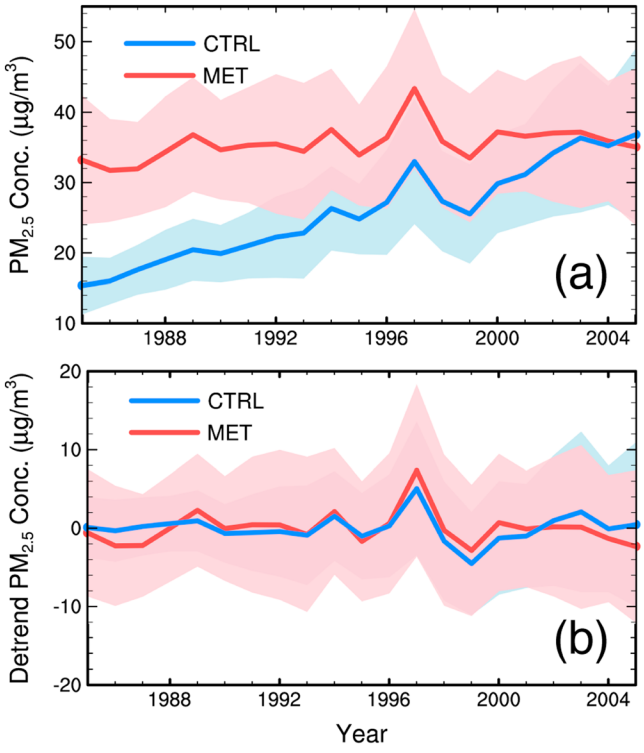

Figure 6. Time series of (a) simulated DJF mean surface-layer $PM_{2.5}$ concentrations averaged over eastern China (105–122.5°E, 20–45°N) for 1985–2005 from the CTRL (blue line) and MET (red line) simulations and (b) the corresponding concentrations after linear trends were removed from the time series (μg m^{-3}). Mean values are shown in lines with $\pm\sigma$ (standard deviation) shown in light color areas in Figures 6a and 6b. Trends in the CTRL and MET simulations (Figure 6a) are both significant at the 95% confidence level from the *F* test on the regression model.

January and February 1998) were probably due to the error in GEOS-4 meteorology in January and February 1998 (http://wiki.seas.harvard.edu/geos-chem/index.php/GMAO_GEOS-4).

Figure 7 shows the linear trends of the simulated concentrations of different aerosol species in DJF from 1985 to 2005 in the CTRL and MET simulations. The increases in aerosol concentrations were simulated over central eastern China, with values in the CTRL simulation an order of magnitude larger than those in the MET simulation. In the CTRL simulation, nitrate aerosol concentrations showed the largest increasing trend, probably because the model overestimates nitrate in eastern China [*Wang et al.*, 2013], followed by sulfate, ammonium, OC, and BC. Sulfate, nitrate, and ammonium increased faster than carbonaceous aerosols, because their precursor emissions increased faster than the emissions of OC and BC (Figure 1). This revealed that sulfate, nitrate, and ammonium became increasingly important in the haze formation over eastern China. It is worth noting that the version of the GEOS-Chem model used in this study does not have the complex secondary organic aerosol simulation; therefore, the decadal increases in $PM_{2.5}$ concentrations may have been underestimated in our simulations.

5. Relative Importance of Each Meteorological Parameter

To estimate the relative contribution of each meteorological parameter to the variations in DJF surface-layer $PM_{2.5}$ concentrations, stepwise linear regressions were used for daily $PM_{2.5}$ concentrations over eastern China (105–122.5°E, 20–45°N), northern China (105–122.5°E, 34–45°N), and southern China (105–122.5°E, 20–34°N) from the MET simulation. The stepwise regression model is in the following form:

$$y = \beta_0 + \sum_{k=1}^{9} \beta_k x_k + \text{interaction terms}$$

where y is normalized daily $PM_{2.5}$ concentration and (x_1, …, x_9) are the ensemble of normalized daily meteorological variables of wind speed at 850 hPa (WINDS), the east-west direction indicator (EW), the north-south direction indicator (NS), planetary boundary layer height (PBLH), surface temperature (TS), surface specific humidity (SH), cloud fraction (CLD), precipitation rate (PREC), and upward flux (UP) in DJF of 1985–2005 from GEOS-4 meteorology. θ is the angle of the horizontal wind vector counterclockwise from the east. EW is cos θ at 850 hPa representing east-west wind direction. NS is sin θ at 850 hPa representing north-south wind direction. The interaction terms (for example, the interaction of the *l*th and *m*th meteorological parameters, $x_l x_m$) are up to second order. The regression coefficient β_k is determined by a stepwise method to add and delete terms to obtain the best model fit [*Venables and Ripley*, 2003; *Tai et al.*, 2010]. Totally, about 26 terms are retained in the stepwise regression with the coefficients of determination (R^2) in the range of 0.55–0.82.

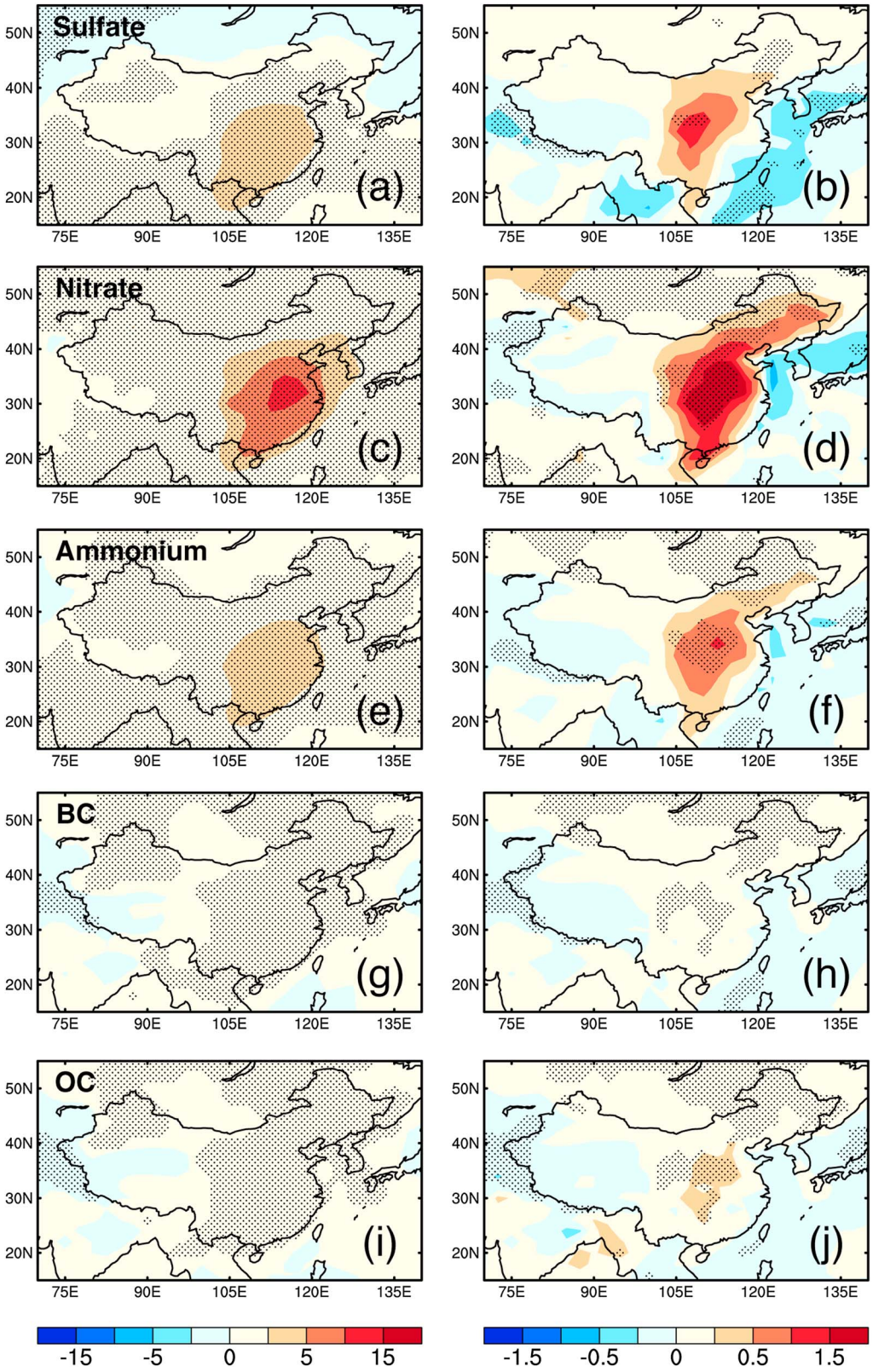

Figure 7. Linear trends in simulated surface-layer (a, b) sulfate, (c, d) nitrate, (e, f) ammonium, (g, h) black carbon, and (i, j) organic carbon concentrations ($\mu g\ m^{-3}\ decade^{-1}$) for 1985–2005 from the CTRL (Figures 7a, 7c, 7e, 7g, and 7i) and MET (Figures 7b, 7d, 7f, 7h, and 7j) simulations. The dotted areas indicate statistical significance at the 95% confidence level from the *F* test on the regression model.

Table 1. Regression Coefficients for Stepwise Linear Regression Models Performed With Spatially Averaged Meteorological Variables and $PM_{2.5}$ Concentrations for Eastern China (105–122.5°E, 20–45°N), Northern China (105–122.5°E, 34–45°N), and Southern China (105–122.5°E, 20–34°N)[a]

Meteorological Parameter	Regression Coefficients		
	Eastern China	Northern China	Southern China
WINDS	−0.35	−0.28	−0.52
EW	−0.09	−0.07	−0.29
NS	0.02	0.25	−0.23
PBLH	−0.31	−0.11	−0.32
TS	0.27	0.14	0.14
SH	0.09	0.53	0.02
CLD	0.15	0.07	0.08
PREC	−0.29	−0.18	−0.27
UP	0.13	0.24	0.17

[a]Regression coefficients were determined by the stepwise method. Regressors include normalized daily wind speed at 850 hPa (WINDS, m s^{-1}), east-west direction indicator cos θ at 850 hPa (EW, dimensionless), north-south direction indicator sin θ at 850 hPa (NS, dimensionless), planetary boundary layer height (PBLH, km), surface temperature (TS, K), surface specific humidity (SH, g kg^{-1}), cloud fraction (CLD, %), precipitation rate (PREC, mm d^{-1}), and upward flux (UP, kg s^{-1}) in DJF derived from GEOS-4 meteorological fields. Daily DJF surface-layer $PM_{2.5}$ concentrations (μg m^{-3}) from the MET simulation were used as the dependent variable of regression model.

Table 1 summarizes the regression coefficients for the stepwise regression models. Over eastern China, the regression coefficient for WINDS was negative; that is, decreases in wind speed led to increases in $PM_{2.5}$ concentrations. This is consistent with previous studies of haze formation over eastern China [*Zhao et al*., 2013; *Li et al*., 2016]. In winter, eastern China is dominated by strong northwesterly winds associated with the East Asian winter monsoon. The positive regression coefficient for NS and the negative regression coefficient for EW over northern China reduced wind speed and obstructed the pollution transported to the downwind area, leading to haze days over northern China. Over southern China, the negative regression coefficient for EW indicated weaker northwesterly winds, and the negative regression coefficient for NS indicated the transport of polluted air from northern to southern China, both leading to higher aerosol concentrations over southern China. With a negative regression coefficient, decreases in PBLH allowed more pollutants to accumulate in the shallow layer, favoring haze formation over eastern China [*Zhao et al*., 2013].

Higher temperatures can lead to increased gas-phase reaction rates and oxidant concentrations, which result in higher sulfate concentrations [*Liao et al*., 2006]. Increasing humidity causes an increase in aerosol water content and hence the uptake of semivolatile components, promoting the formation of ammonium nitrate [*Dawson et al*., 2007]. Sulfate concentration is expected to increase with increasing cloudiness due to increases in aqueous production, but an accompanied increase in precipitation may have the opposite effect due to an increase in wet scavenging [*Pye et al*., 2009]. These previous findings explain the positive regression coefficients of TS, SH, and CLD and the negative regression coefficient of PREC. The upward flux in the model is associated with the convergence of aerosols. The positive regression coefficient of UP indicated the convergence and accumulation of $PM_{2.5}$, which was associated with the occurrence of haze.

To examine the contribution of each meteorological parameter to the increase in $PM_{2.5}$ concentrations, the LMG (Lindeman, Merenda, and Gold) method [*Lindeman et al*., 1980; *Grömping*, 2006] was applied in this study. This method is one of the most state-of-the-art methods for determining the relative importance of correlated attributes [*Grömping*, 2006; *Bi*, 2012] and provides a decomposition of the model-explained variance into nonnegative contributions. This approach has been used in many studies to estimate the relative roles of aerosol and meteorological parameters in variations in cloud radiative effects [*Xu et al*., 2015; *Yang et al*., 2016]. The estimated fractions of variance in DJF mean surface-layer $PM_{2.5}$ concentrations over eastern, northern, and southern China are presented in Figure 8. Horizontal winds (WINDS + EW + NS) were the dominant factor, explaining 37, 35, and 40% of the variance of $PM_{2.5}$ concentrations over eastern, northern, and southern China, respectively. Planetary boundary layer height was the second most important factor, explaining 25% of the variance of $PM_{2.5}$ concentrations over eastern China. It contributed 24% of the variance over southern China and 9% of the variance over northern China. Over northern China, 25% of the variance was also driven by variations in specific humidity. Other meteorological parameters had smaller impacts on the

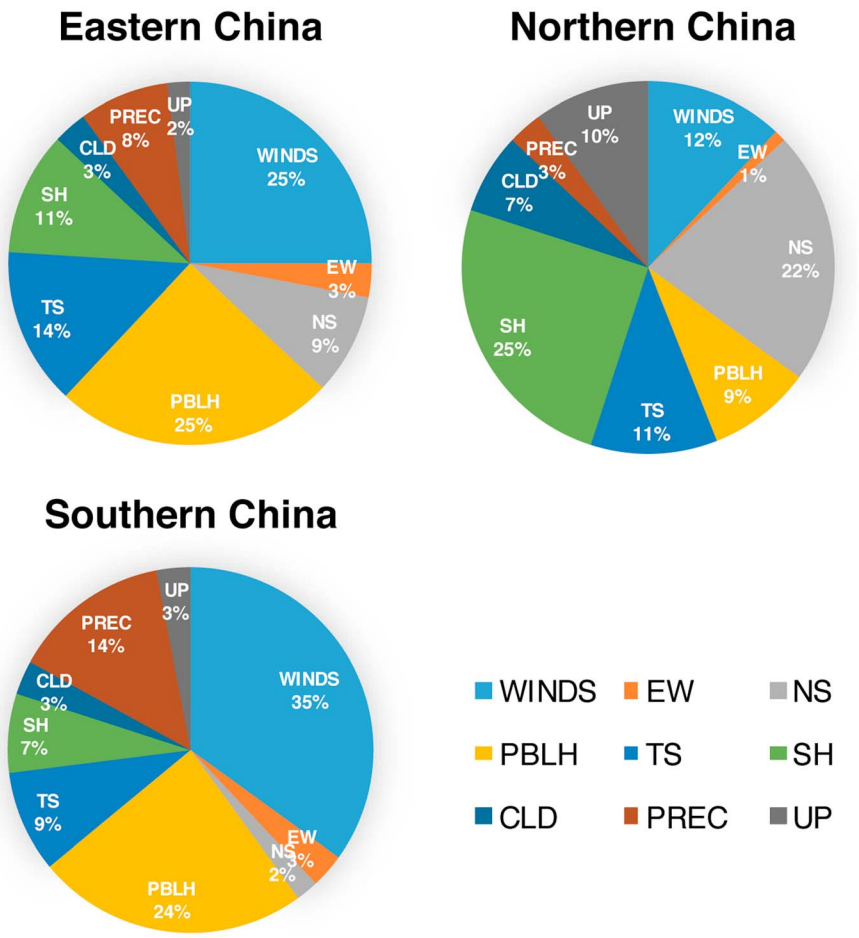

Figure 8. The LMG method for estimated fraction of variance in simulated DJF mean surface-layer $PM_{2.5}$ concentrations over eastern China (105–122.5°E, 20–45°N), northern China (105–122.5°E, 34–45°N), and southern China (105–122.5°E, 20–34°N) from the MET simulation explained by wind speed at 850 hPa (WINDS), east-west direction indicator cos θ at 850 hPa (EW), north-south direction indicator sin θ at 850 hPa (NS), planetary boundary layer height (PBLH), surface temperature (TS), surface specific humidity (SH), cloud fraction (CLD), precipitation rate (PREC), and upward flux (UP). Meteorological parameters were derived from GEOS-4 assimilated meteorological fields.

variance of $PM_{2.5}$ concentrations over eastern China, with contributions less than 20%. Note that the LMG method examined the contributions of meteorological parameters to the variance of $PM_{2.5}$ concentrations, which included all of the decadal, interannual, and daily signals of the variations in $PM_{2.5}$ concentrations. The estimated fraction of variance in different aerosol species over eastern China did not show large changes compared with that of $PM_{2.5}$, with the largest contribution of horizontal wind ranging from 33 to 40% (data not shown). The slight changes in contributions for different meteorological parameters were due to the different spatial distributions and the different sensitivities of aerosols to meteorology.

To confirm the influence of winds on the decadal increasing trend of $PM_{2.5}$ concentrations over eastern China, Figures 9a and 9b show the climatological mean and linear trends of DJF mean horizontal winds at 850 hPa from 1985 to 2005 derived from GEOS-4 meteorological fields. GEOS-4 captures well typical features in winds; that is, the strong northwesterly winds prevail in eastern China, especially in northern China in the East Asian winter monsoon season. During 1985–2005, northerlies became weaker in northern China (Figure 9b), leading to more aerosols accumulating in the atmosphere, which resulted in increasing trends of aerosol concentrations and haze days over northern China. Over the Yangtze River Delta in eastern China, westerly winds also became weaker, resulting in the increase in aerosol concentrations around the 30°N band of eastern China. The increase in anomalous northeasterly winds transported aerosols from the highly polluted Yangtze River Delta to central China, resulting in increasing aerosols over central China for

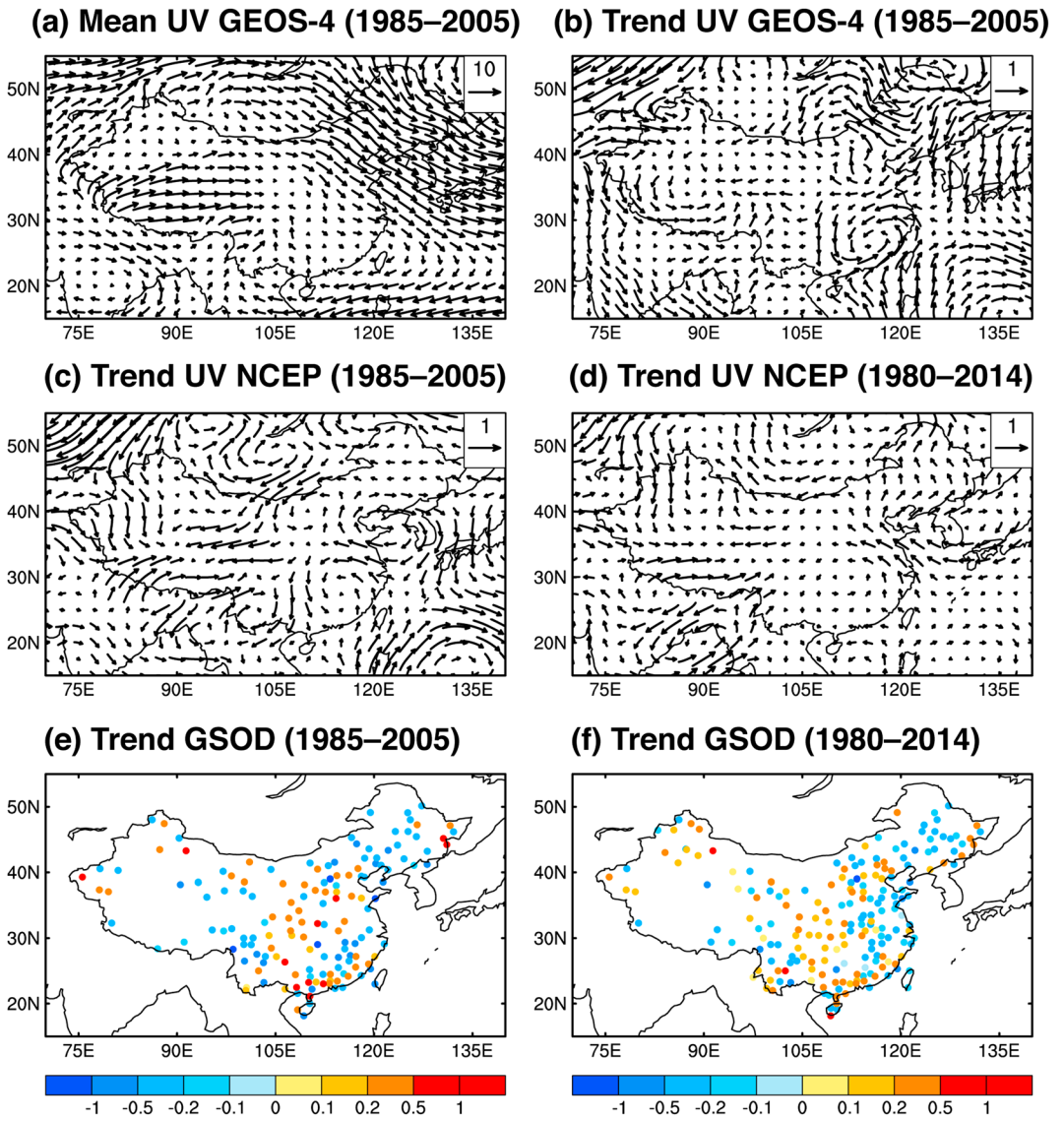

Figure 9. (a) DJF mean of horizontal winds at 850 hPa averaged over 1985–2005 derived from GEOS-4 assimilated meteorological fields (m s^{-1}). The linear trends in horizontal winds at 850 hPa for (b) 1985–2005 derived from the GEOS-4 assimilated meteorological fields, (c) 1985–2005, and (d) 1980–2014 derived from the NCEP/NACR reanalysis data and linear trends in surface-layer wind speed for (e) 1985–2005 and (f) 1980–2014 from the National Climatic Data Center (NCDC) Global Summary of Day (GSOD) database (m s^{-1} $decade^{-1}$). Only stations with trends at the 5% significance level are shown in Figures 9e and 9f.

the winters of 1985–2005. Figure 9c shows the linear trends of DJF mean horizontal winds at 850 hPa for 1985–2005 derived from NCEP/NCAR (National Centers for Environmental Prediction/National Center for Atmospheric Research) reanalysis data. The wind trends from the NCEP/NCAR reanalysis data were almost the same as those from GEOS-4 over the same period of 1985–2005 over eastern China, which confirmed the wind trends in the simulations. Figure 9d also presents the wind trends for the winters of 1980–2014 from the NCEP/NCAR reanalysis data. During the past three decades, northwesterly winds became weaker over northern China and coastal areas in southern China, resulting in the decadal increase in aerosol concentrations and haze days over eastern China. The trend of GEOS-4 wind speed at 850 hPa averaged over eastern China was -0.09 m s^{-1} $decade^{-1}$ over 1985–2005, lower than -0.14 and -0.10 m s^{-1} $decade^{-1}$ from the NCEP/NCAR reanalysis data over 1985–2005 and 1980–2014, respectively, suggesting that the model may underestimate the role of winds in the increasing trend of aerosols.

In addition to the wind trends from the reanalysis in our study, *McVicar et al*. [2012] reviewed the wind speed trend during recent decades and showed a decreasing trend over eastern China in all of the studies they reviewed, which confirms our results. The reduced wind speed is driven by the interplay of many factors, including the weakening of the East Asian monsoon resulting from global warming [*Hu et al*., 2000; *Xu et al*., 2006; *Jiang et al*., 2010; *Guo et al*., 2011], a shift in the dominant mode of the Arctic Oscillation [*He and Wang*, 2013], the variability in North Pacific sea surface temperature [*Sun et al*., 2015], the interdecadal variations of quasi-stationary planetary waves [*L. Wang et al*., 2009], and urbanization [*Li et al*., 2011]. Figures 9e and 9f show the DJF mean surface wind speed trend over 1985–2005 and 1980–2014 from the GSOD database. Over eastern China, especially the coastal areas, more than half of the stations showed statistically significant decreasing trends, in agreement with GEOS-4 and NCEP/NCAR meteorology. The wind speed trend at the surface layer averaged over eastern China from GSOD was −0.09 and $-0.08\,\mathrm{m\,s^{-1}\,decade^{-1}}$ over 1985–2005 and 1980–2014, respectively, almost the same value as that from GEOS-4. Note that we showed wind vectors at 850 hPa for GEOS-4 and NCEP/NCAR data, because aerosol transport is the largest around this layer [*Yang et al*., 2015], whereas the GSOD database only provides wind speed at the surface layer. It should be noted that the results presented here are based on the meteorology derived from the reanalysis data, which may have some biases compared with the observed meteorology.

6. Conclusions and Discussions

The increases in winter haze days and $PM_{2.5}$ concentrations over eastern China over the past few decades were examined using observed atmospheric visibility from the National Climatic Data Center Global Summary of Day database and simulated $PM_{2.5}$ concentrations from the GEOS-Chem model driven by assimilated GEOS-4 meteorological fields. Winter visibility decreased from 15.6 km in 1980 to 12.7 km in 2014, accompanied by an increase in winter haze days from 21.3 to 41.5 days averaged over eastern China. The GEOS-Chem model captured the increasing trend of winter $PM_{2.5}$ concentrations for 1985–2005, with concentrations averaged over eastern China increasing from 16.1 $\mu g\,m^{-3}$ in 1985 to 38.4 $\mu g\,m^{-3}$ in 2005.

Considering the variations in both anthropogenic emissions and meteorological parameters, the model simulated a trend of DJF mean surface-layer $PM_{2.5}$ concentrations of 10.5 (±6.2) $\mu g\,m^{-3}\,decade^{-1}$ averaged over eastern China. Considering the variations in meteorological parameters alone, eastern China showed a smaller increasing trend in $PM_{2.5}$ concentrations, with a statistically significant trend of 1.8 (±1.5) $\mu g\,m^{-3}\,decade^{-1}$. Variations in anthropogenic emissions dominated the increase in winter $PM_{2.5}$ concentrations over eastern China during the past decades. However, variations in meteorological parameters also played an important role in influencing the decadal increase in $PM_{2.5}$ concentrations, which contributed 17 (±14)% to the increasing trend between 1985 and 2005.

Through stepwise linear regressions, the increase in DJF surface-layer $PM_{2.5}$ over eastern China was found to be associated with the decrease in wind speed, eastward winds, planetary boundary layer height, and precipitation rate and the increase in northward winds, surface temperature, specific humidity, cloud fraction, and convergence. The LMG method for linear models suggested that horizontal winds were the dominant factor, explaining 37, 35, and 40% of the variances in $PM_{2.5}$ concentrations over eastern, northern, and southern China.

Further analysis of the trends in meteorological parameters showed that between 1985 and 2005, northerly winds became weaker in northern China, leading to more aerosols accumulating in the atmosphere, which resulted in the increasing trends in aerosol concentrations and haze days over northern China. Over the Yangtze River Delta in eastern China, westerly winds also became weaker, resulting in the increase in aerosol concentrations around the 30°N band of eastern China. The increase in anomalous northeasterly winds transported aerosols from the highly polluted Yangtze River Delta to central China, increasing aerosols and haze days over central China for 1985–2005. Winds with longer time coverage for 1980–2014 from the NCEP/NCAR reanalysis data showed that northwesterly winds became weaker over northern China and the coastal area in southern China, resulting in decadal increases in aerosol concentrations and haze days over eastern China during recent decades.

In this study, the roles of anthropogenic emissions and meteorological fields in the trend of winter haze over eastern China were examined through the GEOS-Chem model simulations. Note that because of the lack of

data sets, the biomass burning emissions were fixed at the 2005 level, which might have led to low biases in the simulated interannual variations of $PM_{2.5}$ concentrations. The version of the GEOS-Chem model used in this study does not have the secondary organic aerosol simulation. If current models were to include secondary organic aerosols, more accurate aerosol and haze trends could be presented. The assimilated GEOS-4 meteorological fields are available for the winters of 1985 to 2005, which were used in this work for consistency with our previous studies that examined interannual and decadal variations of pollutants [*Yang et al.*, 2014, 2015]. A longer time series and more recent meteorology, such as the Modern-Era Retrospective analysis for Research and Applications, should be used in future studies. In addition to the meteorological fields examined in this study, other dynamic and thermodynamic meteorological parameters, such as wind shear and temperature inversion, could also lead to haze occurrence [*Zhang et al.*, 2014]. These issues need to be examined in future studies of haze trend over eastern China.

Acknowledgments

This work was supported by the National Basic Research Program of China (973 program, grant 2014CB441202), the Strategic Priority Research Program of the Chinese Academy of Sciences (grant XDA05100503), and the National Natural Science Foundation of China under grants 91544219 and 41475137. We acknowledge support from the U.S. Department of Energy (DOE), Office of Science, Biological and Environmental Research. The Pacific Northwest National Laboratory (PNNL) is operated for DOE by Battelle Memorial Institute under contract DE-AC05-76RLO1830. The data for these results are posted at China">http://portal.nersc.gov/project/m1374/Haze_China.

References

Alexander, B., R. J. Park, D. J. Jacob, Q. B. Li, R. M. Yantosca, J. Savarino, C. C. W. Lee, and M. H. Thiemens (2005), Sulfate formation in sea-salt aerosols: Constraints from oxygen isotopes, *J. Geophys. Res.*, *110*, D10307, doi:10.1029/2004JD005659.

Bi, J. (2012), A review of statistical methods for determination of relative importance of correlated predictors and identification of drivers of consumer liking, *J. Sens. Stud.*, *27*, 87–101, doi:10.1111/j.1745-459X.2012.00370.x.

Chameides, W. L., et al. (1999), Case study of the effects of atmospheric aerosols and regional haze on agriculture: An opportunity to enhance crop yields in China through emission controls?, *Proc. Natl. Acad. Sci. U.S.A.*, *96*(24), 13,626–13,633.

Chang, D., Y. Song, and B. Liu (2009), Visibility trends in six megacities in China 1973–2007, *Atmos. Res.*, *94*, 161–167, doi:10.1016/j.atmosres.2009.05.006.

Che, H., X. Zhang, Y. Li, Z. Zhou, and J. J. Qu (2007), Horizontal visibility trends in China 1981–2005, *Geophys. Res. Lett.*, *34*, L24706, doi:10.1029/2007GL031450.

Che, H., X. Zhang, Y. Li, Z. Zhou, J. J. Qu, and X. Hao (2009), Haze trends over the capital cities of 31 provinces in China, 1981–2005, *Theor. Appl. Climatol.*, *97*, 235–242, doi:10.1007/s00704-008-0059-8.

Che, H. Z., G. Y. Shi, X. Y. Zhang, R. Arimoto, J. Q. Zhao, L. Xu, B. Wang, and Z. H. Chen (2005), Analysis of 40 years of solar radiation data from China, 1961–2000, *Geophys. Res. Lett.*, *32*, L06803, doi:10.1029/2004GL022322.

Chen, H., and H. Wang (2015), Haze days in North China and the associated atmospheric circulations based on daily visibility data from 1960 to 2012, *J. Geophys. Res. Atmos.*, *120*, 5895–5909, doi:10.1002/2015JD023225.

Chen, Y., and S. Xie (2012), Temporal and spatial visibility trends in the Sichuan Basin, China, 1973 to 2010, *Atmos. Res.*, *112*, 25–34, doi:10.1016/j.atmosres.2012.04.009.

Cheng, Z., S. Wang, J. Jiang, Q. Fu, C. Chen, B. Xu, J. Yu, X. Fu, and J. Hao (2013), Long-term trend of haze pollution and impact of particulate matter in the Yangtze River Delta, China, *Environ. Pollut.*, *182*, 101–110, doi:10.1016/j.envpol.2013.06.043.

Dawson, J. P., P. J. Adams, and S. N. Pandis (2007), Sensitivity of $PM_{2.5}$ to climate in the eastern US: A modeling case study, *Atmos. Chem. Phys.*, *7*(16), 4295–4309, doi:10.5194/acp-7-4295-2007.

Deng, J., K. Du, K. Wang, C. Yuan, and J. Zhao (2012), Long-term atmospheric visibility trend in Southeast China, 1973–2010, *Atmos. Environ.*, *59*, 11–21, doi:10.1016/j.atmosenv.2012.05.023.

Ding, Y. H., and Y. J. Liu (2014), Analysis of long-term variations of fog and haze in China in recent 50 years and their relations with atmospheric humidity, *Sci. China Earth Sci.*, *57*, 36–46, doi:10.1007/s11430-013-4792-1.

Dong, W. X., J. Xing, and S. X. Wang (2010), Temporal and spatial distribution of anthropogenic ammonia emissions in China: 1994–2006, [in Chinese] *Environ. Sci.*, *31*, 1457–1463.

Duan, F., K. He, Y. Ma, F. Yang, X. Yu, S. Cadle, T. Chan, and P. Mulawa (2006), Concentration and chemical characteristics of $PM_{2.5}$ in Beijing, China: 2001–2002, *Sci. Total Environ.*, *355*(1–3), 264–275, doi:10.1016/j.scitotenv.2005.03.001.

Evans, M. J., and D. J. Jacob (2005), Impact of new laboratory studies of N_2O_5 hydrolysis on global model budgets of tropospheric nitrogen oxides, ozone, and OH, *Geophys. Res. Lett.*, *32*, L09813, doi:10.1029/2005GL022469.

Fairlie, T. D., D. J. Jacob, and R. J. Park (2007), The impact of transpacific transport of mineral dust in the United States, *Atmos. Environ.*, *41*(6), 1251–1266, doi:10.1016/j.atmosenv.2006.09.048.

Fajersztajn, L., M. Veras, L. V. Barrozo, and P. Saldiva (2013), Air pollution: A potentially modifiable risk factor for lung cancer, *Nat. Rev. Cancer*, *13*, 674–678, doi:10.1038/nrc3572.

Grömping, U. (2006), Relative importance for linear regression in R: The package relaimpo, *J. Stat. Software*, *17*, 1–27, doi:10.18637/jss.v017.i01.

Guo, H., M. Xu, and Q. Hu (2011), Changes in near-surface wind speed in China: 1969–2005, *Int. J. Climatol.*, *31*, 349–358, doi:10.1002/joc.2091.

Han, X., M. Zhang, J. Tao, L. Wang, J. Gao, S. Wang, and F. Chai (2013), Modeling aerosol impacts on atmospheric visibility in Beijing with RAMS-CMAQ, *Atmos. Environ.*, *72*, 177–191, doi:10.1016/j.atmosenv.2013.02.030.

He, S., and H. Wang (2013), Oscillating relationship between the East Asian winter monsoon and ENSO, *J. Clim.*, *26*, 3377–3393, doi:10.1175/JCLI-D-13-00174.1.

Hu, Z. Z., L. Bengtsson, and K. Arpe (2000), Impact of global warming on the Asian winter monsoon in a coupled GCM, *J. Geophys. Res.*, *105*, 4607–4624, doi:10.1029/1999JD901031.

Jacob, D. J. (2000), Heterogeneous chemistry and tropospheric ozone, *Atmos. Environ.*, *34*, 2131–2159, doi:10.1016/S1352-2310(99)00462-8.

Jeong, J. I., and R. J. Park (2013), Effects of the meteorological variability on regional air quality in East Asia, *Atmos. Environ.*, *69*, 46–55, doi:10.1016/J.Atmosenv.2012.11.061.

Jiang, H., H. Liao, H. O. T. Pye, S. Wu, L. J. Mickley, J. H. Seinfeld, and X. Y. Zhang (2013), Projected effect of 2000–2050 changes in climate and emissions on aerosol levels in China and associated transboundary transport, *Atmos. Chem. Phys.*, *13*, 7937–7960, doi:10.5194/acp-13-7937-2013.

Jiang, Y., Y. Luo, Z. C. Zhao, and S. W. Tao (2010), Changes in wind speed over China during 1956–2004, *Theor. Appl. Climatol.*, *99*, 421–430, doi:10.1007/s00704-009-0152-7.

Kaiser, D. P., and Y. Qian (2002), Decreasing trends in sunshine duration over China for 1954–1998: Indication of increased haze pollution?, *Geophys. Res. Lett.*, *29*(21), 2042, doi:10.1029/2002GL016057.
Lamarque, J. F., et al. (2010), Historical (1850–2000) gridded anthropogenic and biomass burning emissions of reactive gases and aerosols: Methodology and application, *Atmos. Chem. Phys.*, *10*, 7017–7039, doi:10.5194/acp-10-7017-2010.
Li, Q., R. Zhang, and Y. Wang (2016), Interannual variation of the wintertime fog–haze days across central and eastern China and its relation with East Asian winter monsoon, *Int. J. Climatol.*, *36*, 346–354, doi:10.1002/joc.4350.
Li, Z., Z. W. Yan, K. Tu, W. D. Liu, and Y. C. Wang (2011), Changes in wind speed and extremes in Beijing during 1960–2008 based on homogenized observations, *Adv. Atmos. Sci.*, *28*(2), 408–420, doi:10.1007/s00376-010-0018-z.
Liao, H., W.-T. Chen, and J. H. Seinfeld (2006), Role of climate change in global predictions of future tropospheric ozone and aerosols, *J. Geophys. Res.*, *111*, D12304, doi:10.1029/2005JD006852.
Liao, H., W. Chang, and Y. Yang (2015), Climatic effects of air pollutants over China: A review, *Adv. Atmos. Sci.*, *32*(1), 115–139, doi:10.1007/s00376-014-0013-x.
Lim, S. S., et al. (2012), A comparative risk assessment of burden of disease and injury attributable to 67 risk factors and risk factor clusters in 21 regions, 1990–2010: A systematic analysis for the Global Burden of Disease Study 2010, *Lancet*, *380*, 2224–2260, doi:10.1016/S0140-6736(12)61766-8.
Lindeman, R. H., P. F. Merenda, and R. Z. Gold (1980), *Introduction to Bivariate and Multivariate Analysis*, Scott, Foresman, Glenview, Ill.
Lou, S., H. Liao, and B. Zhu (2014), Impacts of aerosols on surface-layer ozone concentrations in China through heterogeneous reactions and changes in photolysis rates, *Atmos. Environ.*, *85*, 123–138, doi:10.1016/j.atmosenv.2013.12.004.
Lu, Z., Q. Zhang, and D. G. Streets (2011), Sulfur dioxide and primary carbonaceous aerosol emissions in China and India, 1996–2010, *Atmos. Chem. Phys.*, *11*, 9839–9864, doi:10.5194/acp-11-9839-2011.
McVicar, T. R., et al. (2012), Global review and synthesis of trends in observed terrestrial near-surface wind speed: Implications for evaporation, *J. Hydrol.*, *416–417*, 182–205, doi:10.1016/j.jhydrol.2011.10.024.
Nenes, A., C. Pilinis, and S. N. Pandis (1998), ISORROPIA: A new thermodynamic model for multiphase multicomponent inorganic aerosols, *Aquat. Geochem.*, *4*, 123–152.
Park, F. J. (2004), Natural and transboundary pollution influences on sulfate-nitrate-ammonium aerosols in the United States: Implications for policy, *J. Geophys. Res.*, *109*, D15204, doi:10.1029/2003JD004473.
Park, R. J., D. J. Jacob, M. Chin, and R. V. Martin (2003), Sources of carbonaceous aerosols over the United States and implications for natural visibility, *J. Geophys. Res.*, *108*(D12), 4355, doi:10.1029/2002JD003190.
Park, R. J., D. J. Jacob, B. D. Field, R. M. Yantosca, and M. Chin (2004), Natural and transboundary pollution influences on sulfate-nitrate-ammonium aerosols in the United States: Implications for policy, *J. Geophys. Res.*, *109*, D15204, doi:10.1029/2003JD004473.
Peplow, M. (2014), Beijing smog contains witches' brew of microbes, *Nature*, doi:10.1038/nature.2014.14640.
Pye, H. O. T., H. Liao, S. Wu, L. J. Mickley, D. J. Jacob, D. K. Henze, and J. H. Seinfeld (2009), Effect of changes in climate and emissions on future sulfate-nitrate-ammonium aerosol levels in the United States, *J. Geophys. Res.*, *114*, D01205, doi:10.1029/2008JD010701.
Qian, Y., and F. Giorgi (2000), Regional climatic effects of anthropogenic aerosols? The case of Southwestern China, *Geophys. Res. Lett.*, *27*, 3521–3524, doi:10.1029/2000GL011942.
Streets, D. G., et al. (2003), An inventory of gaseous and primary aerosol emissions in Asia in the year 2000, *J. Geophys. Res.*, *108*(D21), 8809, doi:10.1029/2002JD003093.
Sun, J., S. Wu, and J. Ao (2015), Role of the North Pacific sea surface temperature in the East Asian winter monsoon decadal variability, *Clim. Dyn.*, doi:10.1007/s00382-015-2805-9.
Sun, Y., Q. Jiang, Z. Wang, P. Fu, J. Li, T. Yang, and Y. Yin (2014), Investigation of the sources and evolution processes of severe haze pollution in Beijing in January 2013, *J. Geophys. Res. Atmos.*, *119*, 4380–4398, doi:10.1002/2014JD021641.
Tai, A. P. K., L. J. Mickley, and D. J. Jacob (2010), Correlations between fine particulate matter ($PM_{2.5}$) and meteorological variables in the United States: Implications for the sensitivity of $PM_{2.5}$ to climate change, *Atmos. Environ.*, *44*, 3976–3984, doi:10.1016/j.atmosenv.2010.06.060.
Thornton, J. A., L. Jaegle, and V. F. McNeill (2008), Assessing known pathways for HO_2 loss in aqueous atmospheric aerosols: Regional and global impacts on tropospheric oxidants, *J. Geophys. Res.*, *113*, D05303, doi:10.1029/2007JD009236.
van der Werf, G. R., J. T. Randerson, L. Giglio, G. J. Collatz, P. S. Kasibhatla, and A. F. Arellano Jr. (2006), Interannual variability in global biomass burning emissions from 1997 to 2004, *Atmos. Chem. Phys.*, *6*, 3423–3441, doi:10.5194/acp-6-3423-2006.
van Donkelaar, A., et al. (2008), Analysis of aircraft and satellite measurements from the Intercontinental Chemical Transport Experiment (INTEX-B) to quantify long- range transport of East Asian sulfur to Canada, *Atmos. Chem. Phys.*, *8*, 2999–3014, doi:10.5194/acp-8-2999-2008.
van Donkelaar, A., R. V. Martin, M. Brauer, R. Kahn, R. Levy, C. Verduzco, and P. Villeneuve (2010), Global estimates of average ground-level fine particulate matter concentrations from satellite-based aerosol optical depth, *Environ. Health Perspect.*, *118*, 847–855, doi:10.1289/ehp.0901623.
Venables, W. N., and B. D. Ripley (2003), *Modern Applied Statistics With S*, Springer, New York.
Wang, K., R. E. Dickinson, and S. Liang (2009), Clear sky visibility has decreased over land globally from 1973 to 2007, *Science*, *323*(5920), 1468–1470, doi:10.1126/science.1167549.
Wang, L., R. Huang, L. Gu, W. Chen, and L. Kang (2009), Interdecadal variations of the East Asian winter monsoon and their association with quasi-stationary planetary wave activity, *J. Clim.*, *22*(18), 4860–4872, doi:10.1175/2009JCLI2973.1.
Wang, L. T., Z. Wei, J. Yang, Y. Zhang, F. F. Zhang, J. Su, C. C. Meng, and Q. Zhang (2014), The 2013 severe haze over southern Hebei, China: Model evaluation, source apportionment, and policy implications, *Atmos. Chem. Phys.*, *14*, 3151–3173, doi:10.5194/acp-14-3151-2014.
Wang, Y., Q. Q. Zhang, K. He, Q. Zhang, and L. Chai (2013), Sulfate-nitrate-ammonium aerosols over China: Response to 2000–2015 emission changes of sulfur dioxide, nitrogen oxides, and ammonia, *Atmos. Chem. Phys.*, *13*, 2635–2652, doi:10.5194/acp-13-2635-2013.
Wang, Y., Q. Q. Zhang, J. Jiang, W. Zhou, B. Wang, K. He, F. Duan, Q. Zhang, S. Philip, and Y. Xie (2014), Enhanced sulfate formation during China's severe winter haze episode in January 2013 missing from current models, *J. Geophys. Res. Atmos.*, *119*, 10,425–10,440, doi:10.1002/2013JD021426.
Wang, Y. S., L. Yao, L. L. Wang, Z. R. Liu, D. S. Ji, G. Q. Tang, J. K. Zhang, Y. Sun, B. Hu, and J. Y. Xin (2014), Mechanism for the formation of the January 2013 heavy haze pollution episode over central and eastern China, *Sci. China Earth Sci.*, *57*(1), 14–25, doi:10.1007/s11430-013-4773-4.
Wu, D., X. Tie, C. C. Li, Z. M. Ying, A. K. Lau, J. Huang, X. J. Deng, and X. Y. Bi (2005), An extremely low visibility event over the Guangzhou region: A case study, *Atmos. Environ.*, *39*, 6568–6577, doi:10.1016/j.atmosenv.2005.07.061.

Xu, L., D. W. Pierce, L. M. Russell, A. J. Miller, R. C. J. Somerville, C. H. Twohy, S. J. Ghan, B. Singh, J. Yoon, and P. J. Rasch (2015), Interannual to decadal climate variability of sea salt aerosols in the coupled climate model CESM1.0, *J. Geophys. Res. Atmos.*, *120*, 1502–1519, doi:10.1002/2014JD022888.

Xu, M., C.-P. Chang, C. Fu, Y. Qi, A. Robock, D. Robinson, and H. Zhang (2006), Steady decline of East Asian monsoon winds, 1969–2000: Evidence from direct ground measurements of wind speed, *J. Geophys. Res.*, *111*, D24111, doi:10.1029/2006JD007337.

Xuan, J., G. Liu, and K. Du (2000), Dust emission inventory in northern China, *Atmos. Environ.*, *34*(26), 4565–4570, doi:10.1016/S1352-2310(00)00203-X.

Yang, Y., H. Liao, and J. Li (2014), Impacts of the East Asian summer monsoon on interannual variations of summertime surface-layer ozone concentrations over China, *Atmos. Chem. Phys.*, *14*, 6867–6880, doi:10.5194/acp-14-6867-2014.

Yang, Y., H. Liao, and S. Lou (2015), Decadal trend and interannual variation of outflow of aerosols from East Asia: Roles of variations in meteorological parameters and emissions, *Atmos. Environ.*, *100*, 141–153, doi:10.1016/j.atmosenv.2014.11.004.

Yang, Y., et al. (2016), Impacts of ENSO events on cloud radiative effects in preindustrial conditions: Changes in cloud fraction and their dependence on interactive aerosol emissions and concentrations, *J. Geophys. Res. Atmos.*, *121*, 6321–6335, doi:10.1002/2015JD024503.

Ye, B., X. Ji, H. Yang, X. Yao, C. K. Chan, S. H. Cadle, T. Chan, and P. A. Mulawa (2003), Concentration and chemical composition of $PM_{2.5}$ in Shanghai for a 1-year period, *Atmos. Environ.*, *37*(4), 499–510, doi:10.1016/S1352-2310(02)00918-4.

Zhang, L., H. Liao, and J. Li (2010), Impacts of Asian summer monsoon on seasonal and interannual variations of aerosols over eastern China, *J. Geophys. Res.*, *115*, D00K05, doi:10.1029/2009JD012299.

Zhang, Q., et al. (2009), Asian emissions in 2006 for the NASA INTEX-B mission, *Atmos. Chem. Phys.*, *9*, 5131–5153, doi:10.5194/acp-9-5131-2009.

Zhang, R. H., Q. Li, and R. N. Zhang (2014), Meteorological conditions for the persistent severe fog and haze event over eastern China in January 2013, *Sci. China Earth Sci.*, *57*(1), 26–35, doi:10.1007/s11430-013-4774-3.

Zhao, P., X. Zhang, X. Xu, and X. Zhao (2011), Long-term visibility trends and characteristics in the region of Beijing, Tianjin, and Hebei, China, *Atmos. Res.*, *101*, 711–718, doi:10.1016/j.atmosres.2011.04.019.

Zhao, X. J., P. S. Zhao, J. Xu, W. Meng, W. W. Pu, F. Dong, D. He, and Q. F. Shi (2013), Analysis of a winter regional haze event and its formation mechanism in the North China Plain, *Atmos. Chem. Phys.*, *13*, 5685–5696, doi:10.5194/acp-13-5685-2013.

Zheng, G. J., et al. (2015), Exploring the severe winter haze in Beijing: The impact of synoptic weather, regional transport and heterogeneous reactions, *Atmos. Chem. Phys.*, *15*, 2969–2983, doi:10.5194/acp-15-2969-2015.